OFFPRINT

Drop propulsion in tapered tubes

P. Renvoisé, J. W. M. Bush, M. Prakash and D. Quéré

Please visit the new website
www.epljournal.org

Drop propulsion in tapered tubes

P. Renvoisé[1], J. W. M. Bush[1], M. Prakash[2] and D. Quéré[3]

[1] *Department of Mathematics, MIT - 77 Massachusetts Avenue, Cambridge, MA 02139, USA*
[2] *Center for Bits and Atoms, MIT - 20 Ames Street, Cambridge, MA 02139, USA*
[3] *PMMH, UMR 7636 du CNRS, ESPCI - 10 rue Vauquelin, 75005 Paris, France, EU*

Abstract – We present the results of a combined experimental and theoretical investigation of the motion of wetting droplets in tapered capillary tubes. We demonstrate that drops may move spontaneously towards the tapered end owing to the Laplace pressure gradient established along their length. The influence of gravity on this spontaneous motion is examined by studying drop motion along a tilted tube with its tapered end pointing upwards. Provided the tube taper varies, an equilibrium height may be achieved in which the capillary force is balanced by the drop's weight. We deduce the family of tube shapes that support a stable equilibrium.

Introduction. – In 1712, Hauksbee observed that a drop of orange oil bridging two non-parallel plates propels itself in the direction of maximum confinement, that is, into the gap [1]. The drop asymmetry is responsible for the motion: this wetting liquid meets the plates with a different curvature on its leading and trailing edges, so that a differential Laplace pressure is established between the drop extremities and drives the liquid to the region of maximum confinement. A similar motion takes place in a tapered tube [2], a geometry that will be the subject of our investigation. Related curvature-driven motions may also arise for wetting drops on conical fibers, for which the sign of the curvature is reversed, so that the drop is propelled away from the cone tip [3].

For multiphase flow in natural porous media, constrictions or enlargements of the pore channels will necessarily generate displacement and reconfiguration of drops or bubbles. Such geometries also exist in man-made microfluidic devices, and can be used to control the topology and dynamics of two-phase systems, such as emulsions or foams [4]. Finally, the motion of drops in confined geometries arises in the biological world; for example, a class of shorebirds transport prey-laden water droplets mouthward by opening and closing their beaks in a tweezering motion [5–7].

We here study the behaviour of liquid slugs in tapered tubes. If inserted into a fluid bath, conical tubes cause the liquid to rise via capillary action [8,9], but Tsori demonstrated that even this simple system displays surprisingly rich behaviour [10,11]. For example, a wetting liquid either rises to a finite height, or to the top of the tube if the cone angle exceeds a critical value. Here we consider a wetting drop initially placed in the widest part of an inclined tapered tube, and examine the equilibrium position of the drop. While one might first expect this equilibrium to be obtainable directly from Laplace's formula, we here demonstrate that it is potentially unstable, and that its very existence depends on the detailed shape of the tube.

Initial observations. – We consider drops (or slugs) in tapered tubes that are open at both ends. The tubes are thin relative to the capillary length, so that the menisci bounding the slugs can be considered hemispherical. The liquid wets the solid and meets it with zero contact angle. This condition implies that nanoscopic wetting films develop and progress ahead of the menisci, eliminating contact angle hysteresis, and so favouring drop motion in response to forces. Here, the forces driving motion are gravity and the capillary force arising from the curvature difference of the two menisci, as follows from the tube's tapered geometry. The cone opening angle α will be taken small relative to unity. One expects capillary-induced slug motion in a tilted tube to be eventually halted by gravity, as shown in fig. 1. Our experiment consists of determining when a drop equilibrium position exists, then measuring the position z_o, as a function of the tube shape and tilt angle.

Our capillary cones were created by heating and pulling glass capillary tubes. By fixing a given load at the tube extremity, we generate a constant force that draws and
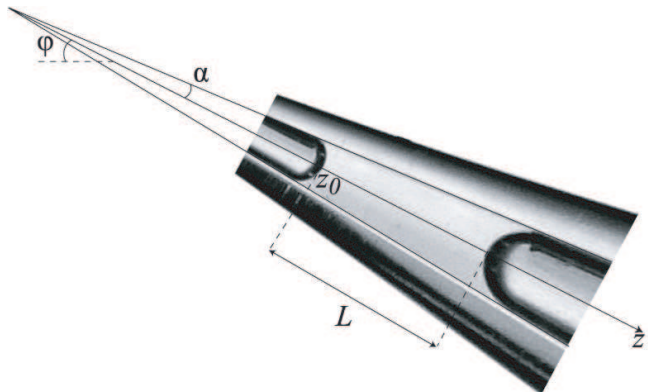
Fig. 1: Drops in tapered tubes can self-propel and eventually stop when the driving capillary force is balanced by gravity. The equilibrium position of the leading edge is denoted by z_o, where the tube tip is taken as the origin, $z = 0$. The slug length is $L(z)$, the cone slope $\alpha(z)$ and the tube tilt angle φ.

thins the hot tube, thus generating a taper. Note that this process does not produce precisely conical tubes (with constant α), a point later shown to be of crucial importance. The liquid used is silicone oil, of surface tension $\gamma = 18\,\mathrm{mN/m}$, density $\rho = 815\,\mathrm{kg/m^3}$ and kinematic viscosity $\nu = 1\,\mathrm{mm^2/s}$. Silicone oils completely wet glass. Observing the menisci through the tube produces image distortion due to the parallax associated with the tube curvature (fig. 1). To avoid such complications, we housed the cones inside channels of square section filled with glycerol, which has a refractive index close to that of the glass and so eliminates parallax. Images were taken by using the macro-mode of a camera and backlighting to enhance the contrast (fig. 2).

The volume Ω of oil introduced at the base of the conical tube varied between 1 and $10\,\mu\mathrm{L}$, and the slope α of the tapered tubes between 0.5 and $5°$. For some tubes, drops were observed to rise to the tip. However, it often happened that the drops stopped at a distance z_o from the tip, as defined in fig. 1, for a given tilt angle φ. In fig. 3, we report the dependence of the equilibrium distance z_o on the drop volume Ω, in a given tapered tube tilted by $\varphi = 30°$ relative to the horizontal. The typical opening angle α in this cone is $5°$. The distance z_o is observed to be a few centimeters, and remarkably it does not depend on Ω over the range of volumes explored.

Conical tubes. – At equilibrium, the liquid weight is balanced by the capillary force arising from the asymmetry of the drop. We assume that the drop length remains small relative to its distance to the tip z ($L \ll z$), and consider tapered tubes of small opening angle ($\alpha \ll 1$). Thus, the drop volume can be written as $\Omega \approx \pi\alpha^2 z^2 L$, and the weight $W \approx \pi\alpha^2 \rho g z^2 L \sin\varphi$. The capillary force is generated by the difference in the radii of curvature of the slug menisci, αz and $\alpha(z + L)$, respectively. Hence, there exists a capillary pressure difference of $2\gamma L/\alpha z^2$ across

the drop, and a Laplace pressure gradient of $2\gamma/\alpha z^2$, which when integrated over the volume produces a force $F \approx 2\pi\gamma\alpha L$. Balancing F with W yields the equilibrium position z_o of the drop:

$$z_o \approx \kappa^{-1}(2/\alpha \sin\varphi)^{1/2}, \qquad (1)$$

where $\kappa^{-1} = (\gamma/\rho g)^{1/2}$ is the capillary length. κ^{-1} is $1.5\,\mathrm{mm}$ for silicone oil, and α is a few degrees, so we expect z_o to be centimetric and independent of the drop volume, as observed in fig. 3.

It is instructive to consider the energy E of the drop. E is the sum of the gravitational and surface energies, and can be expressed as a function of the drop position z. For a wetting liquid, the surface energy arises from two contributions. First, the menisci have a total surface area $4\pi\alpha^2 z^2$ (for $L \ll z$), corresponding to a surface energy $4\pi\gamma\alpha^2 z^2$ that decreases as the drop approaches the tube tip. Second, the tube is covered by a nanoscopic wetting film whose surface area decreases with increasing slug length (*i.e.* decreasing z). The drop contacts the tube on a surface area $2\pi\alpha z L$, or equivalently $2\Omega/(\alpha z)$. In the limit of small opening angles ($\alpha z < L$), the contribution made to the surface energy by the menisci is negligible relative to the change in wetting energy, and the total energy of the system may be expressed to leading order in $\alpha z/L$ as

$$E(z) \approx -\rho g\Omega z \sin\varphi - 2\gamma\Omega/(\alpha z). \qquad (2)$$

Finding the extremum of $E(z)$ yields the equilibrium position z_o defined in eq. (1). However, since E is maximum at z_o, this equilibrium is necessarily unstable. This feature is markedly different from drops on a planar substrate propelled by temperature or chemical gradients, for which tilting the substrate results in a stable-equilibrium position from which one may readily infer the magnitude of the capillary force [12].

Capillary trumpets. – A question naturally arises in light of our experiments. How was it possible to observe in many cases equilibrium positions for the drops (figs. 1 and 3)? The answer lies in the tube shape: while conical tubes have no stable equilibrium, splayed tubes may do. If the tube walls become parallel above the equilibrium position ($z < z_o$), the drop will not move upwards, because the local capillary force vanishes with α; similarly, if the tube splays below z_o, the liquid may be sustained by a strong capillary force at z_o and so avoid falling down.

We proceed by considering trumpet-shaped tubes, whose inner radius a is defined by $a(z) = \delta + \alpha z + \beta z^2$. We again assume that $L \ll z$, and further assume a sufficiently small splay that $\delta > \alpha z + \beta z^2$, a condition fulfilled in the experiments (for which $\beta < 5\,\mathrm{m^{-1}}$. In this limit, the volume can be written as $\Omega \approx \pi\delta^2 L$. Finally, L will be sufficiently large that the volume of liquid in the menisci may be neglected, which for a drop of volume $\Omega = 3\,\mathrm{mm^3}$ is ensured provided $\delta < 0.7\,\mathrm{mm}$, another condition fulfilled in the experiments.
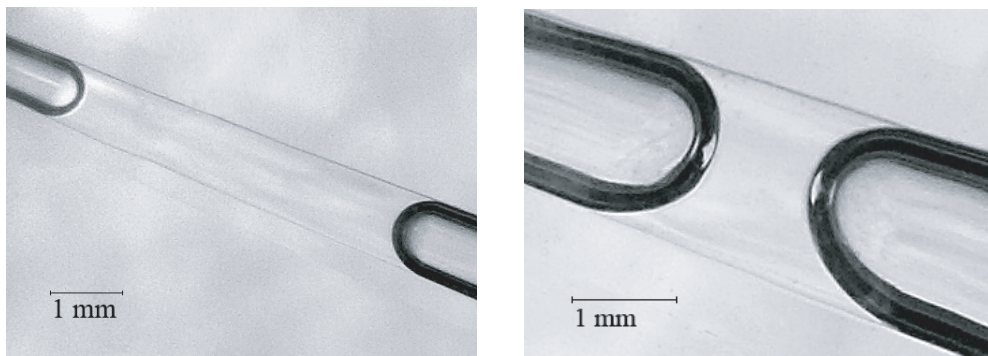
Fig. 2: Fluid slugs of wetting silicone oil, whose capillary length κ^{-1} is 1.5 mm. For sufficiently thin tubes (radius smaller than κ^{-1}), the menisci assume a hemispherical form (a). For larger tubes, asymmetric distortions appear due to gravity (b). Gravity points downward.
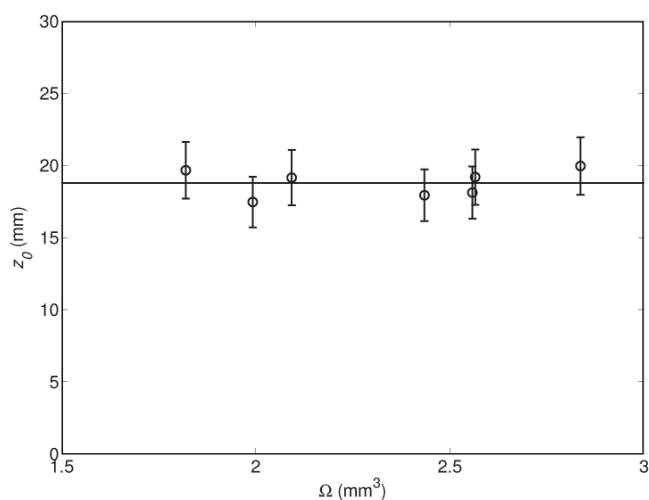

Fig. 3: Equilibrium position z_o of drops of silicone oil placed in a tapered glass tube, inclined at an angle $\varphi = 30 \pm 5°$ relative to the horizontal, as a function of the drop volume Ω. The equilibrium position is independent of the drop volume.
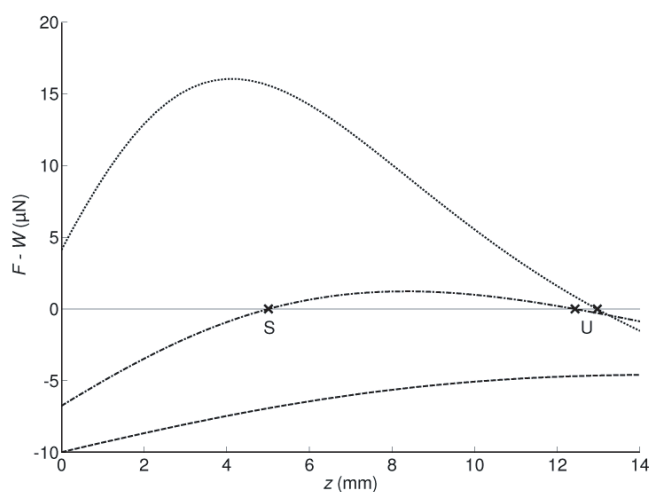

Fig. 4: The net force on the drop, specifically, the difference between the capillary force F and drop weight W, for a drop of volume $\Omega = 3\,\mathrm{mm}^3$ placed in a capillary trumpet inclined at an angle $\varphi = 30°$. The inner radius of the tube is $a(z) = \delta + z^2$ with $\delta = 0.3$ mm and three possible values of the splay β: $\beta = 0.5\,\mathrm{m}^{-1}$ (bottom curve), $\beta = 1.3\,\mathrm{m}^{-1}$ (middle curve), $\beta = 4\,\mathrm{m}^{-1}$ (upper curve). Equilibrium, either stable (S) or unstable (U), is only possible if the splay is sufficiently large, and stable equilibria only arise at intermediate values of β.

We focus on the case $\alpha = 0$, so that the tube radius is given by $a(z) = \delta + \beta z^2$, but return to the more general quadratic form in the appendix. The dependence of the capillary force $F(z) = \mathrm{d}E/\mathrm{d}z$ on drop position z is readily calculated, and the drop's ability to climb is assessed by comparing $F(z)$ to the drop weight $W = \pi \rho g \delta^2 L \sin\varphi$. Figure 4 indicates the z-dependence of the net force, $F(z) - W$, on a drop in a quadratic tube inclined at an angle $\varphi = 30°$ relative to the horizontal. Three values for the tube splay β are considered.

When β is small (bottom curve), the weight always exceeds the capillary force: there is no equilibrium height and the drop falls to the bottom of the tube. In this case, the tube is too close to a cylinder to allow any upward motion. When β is intermediate (middle curve), two equilibrium positions arise, the stability of which are determined by the local sign of $\mathrm{d}F/\mathrm{d}z$. When $\mathrm{d}F/\mathrm{d}z$ is positive, the drop is brought back to equilibrium when perturbed, corresponding to a stable equilibrium (S). We

note that only the higher of the two equilibrium positions (i.e. that of smaller z) is stable. For large β, only an unstable equilibrium (U) arises: the capillary force is enhanced by the large tube splay, so the drop climbs until reaching the top of the tube.

In fig. 5, we present a phase diagram indicating the different drop behaviors as a function of the tube geometry. For the sake of similarity to our experiments, we consider drops of millimetric size ($\Omega = 3\,\mathrm{mm}^3$) and tubes tilted by $\varphi = 30°$. The three regimes correspond to those described in fig. 4. For a given δ and increasing β, i.e. for a cylindrical tube that gets progressively more splayed, we define two values $\beta_{\min}$ and $\beta_{\max}$ that bound the three cases. For $\beta < \beta_{\min}$ the tube is too parallel for the drop to climb (zone I). For $\beta > \beta_{\max}$, the splay of the tube is
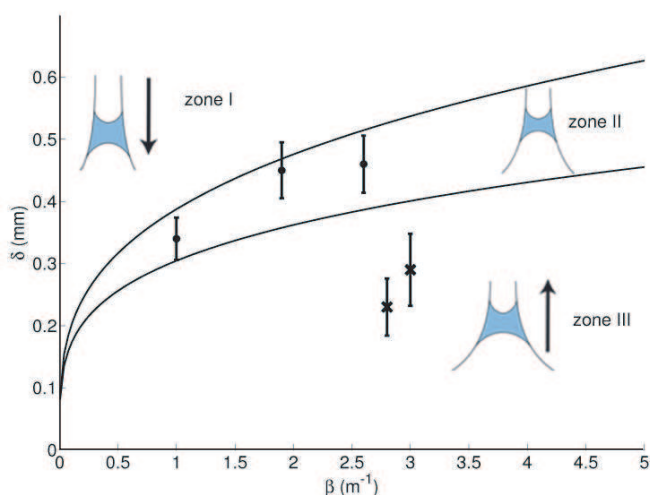
Fig. 5: (Colour on-line) Stability diagram of wetting drops of volume $\Omega = 3\,\text{mm}^3$ placed in a trumpet-shaped tube of inner radius $a(z) = \delta + z^2$ inclined at an angle $30°$ relative to the horizontal. In zone III, the drop always climbs, propelled upwards by the capillary force arising from the large splay of the tube. In zone I, the drop slides downward: owing to relatively wide aperture δ, the weight dominates the capillary force. A stable equilibrium is only possible in zone II. We include in the figure examples of our experimental parameters, and indicate whether drops stopped in the tube (dots), or rose to the top (crosses).

Fig. 6: Equilibrium position z_o of drops of silicone oil inside inclined capillary trumpets of inner radius $a(z) = \delta + z^2$, as a function of the quantity $\delta^2 \sin\varphi/\beta$ which depends on the tube splay β, the tip width δ and the tilt angle φ. As expected from eq. (4), the data collapse onto a single line, whose slope, $0.106 \pm 0.010\,\text{mm}^{-2}$, is close to the anticipated value $\kappa^2/4 = 0.111\,\text{mm}^{-2}$. The data were obtained by varying δ between 0.1 and 0.6 mm, φ between 1 and $50°$ and β between 0.1 and $5\,\text{m}^{-1}$.

so large that the drop can only climb (zone III). Between these extreme values, $\beta_{\min} < \beta < \beta_{\max}$, the drop can reach a stable-equilibrium position (zone II). The boundary between zones II and III is given by $z_o = 0$, and so deduced by solving the equation $F(0) = W$, which yields

$$\delta = (2\kappa^{-2}\Omega\beta/\pi \sin\varphi)^{1/4}. \qquad (3)$$

The boundary between zones I and II is determined numerically, for a given δ, by finding β such that the maximum of the curve $F - W$ (in fig. 4) is zero.

Discussion. – In our experiments, we observed stable-equilibrium positions for wetting drops in tapered tubes (figs. 1 and 3). However, our theoretical investigation indicates that such equilibria are only possible by virtue of a finite tube splay. Our relatively crude fabrication technique inevitably induces such splays: the inner radius of our tubes can be written $\alpha = \delta + \beta z^2$, with typical β-values between 1 and $3\,\text{m}^{-1}$ and δ-values between 0.2 and 0.5 mm. For typical drop volumes ($\Omega = 3\,\text{mm}^3$), and tilt angles ($30°$) considered experimentally, stable-equilibrium positions are anticipated. Figure 5 indicates that the observed drop behaviour, specifically their tendency either to climb in the tube or reach a stable equilibrium, is consistent with our predictions.

In the limits considered in our model, the Laplace pressure difference between the ends of the drop can be written $4\gamma\beta zL/\delta^2$. Integrating over the surface area $\pi\delta^2$ of the tubes yields a capillary force $4\pi\gamma\beta zL$. Balancing
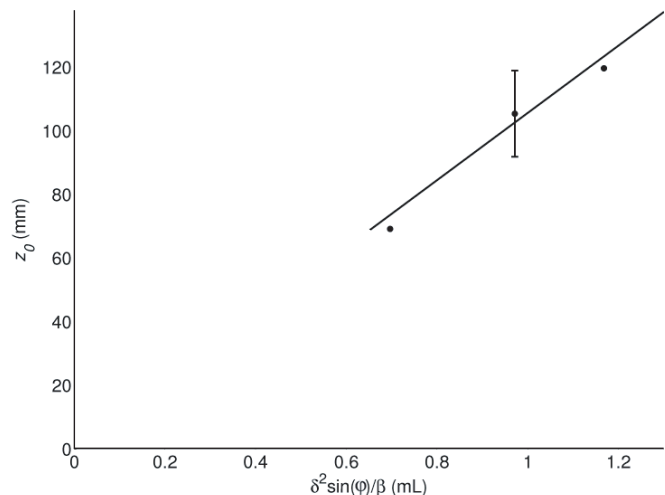
this force with the drop weight $W \approx \pi\rho g\delta^2 L\sin\varphi$ leads to an equilibrium height:

$$z_o \approx \delta^2 \kappa^2 \sin\varphi/4\beta. \qquad (4)$$

This form clearly indicates that the equilibrium position can be fixed by the trumpet geometry: a large splay (β large) favours small z_o (the drop climbs towards the tip), while a wide tip (δ large) favours the fall of the drop (large z_o). For typical values of these parameters, z_o is expected to be centimetric and independent of the drop volume, as observed in fig. 3.

A more quantitative comparison between experiments and eq. (4) can be done by collecting all our data, and plotting the measured z_o as a function of the quantity $\delta^2 \sin\varphi/\beta$ (which has the dimension of a volume) that characterises the trumpet shape and inclination. The data were obtained by varying φ between 1 and $50°$, β between 0.1 and $5\,\text{m}^{-1}$ and δ between 0.1 and 0.6 mm. Figure 6 shows that all the data collapse onto a straight line with slope $0.106 \pm 0.010\,\text{mm}^{-2}$, in excellent agreement with the value $\kappa^2/4 = 0.111\,\text{mm}^{-2}$ anticipated from eq. (4).

We have demonstrated that wetting drops in a tapered capillary tube have a tendency to climb under the influence of capillary action. Depending on tube shape, liquid placed at the base of the tube may either remain stationary, climb until reaching an equilibrium position, or be drawn upwards to the top of the tube. Examining the range of validity of the phase diagrams presented in figs. 5 and 7 requires a careful experimental study that is left as a subject of future research.

The discussion can be extended to partially wetting drops. In this case, the capillary force (per unit length)

along the length of the tube becomes $\gamma\cos\theta$, instead of γ, where θ denotes the contact angle between solid and liquid. This leads in eq. (4) to equilibrium positions, $z_\theta = z_o/\cos\theta$, that are further from the tip than in the case of complete wetting. However, partial wetting is generally accompanied by contact angle hysteresis, which opposes all propulsive forces and so tends to pin the drop. The pinning force arising from a hysteresis $\Delta\cos\theta$ is $2\pi\gamma\delta\Delta\cos\theta$, which dominates the capillary force if $\Delta\cos\theta$ is larger than approximately $\beta z L/\delta$. This is typically expected to be true: $\Delta\cos\theta$ is an order one quantity, while $\beta z L/\delta$ is typically between 0.01 and 0.1 in our study. The capillary force that might otherwise propel partially wetting droplets in tapered tubes is thus likely to be overcome by contact angle hysteresis. This justifies a posteriori our choice of wetting liquids, which not only maximizes the capillary force, but eliminates contact angle hysteresis. We further note that non-wetting liquids ($\theta > 90°$) will tend to produce motion in the direction opposite that considered here, due to the change of sign of the menisci curvatures. For bubbles in a wetting liquid, both the gravity and curvature are reversed, so that we expect our discussion (for example, eq. (4)) to be valid.

Finally, our study suggests new directions in the design of porous solids, on which conical apertures might serve either to promote or resist drop penetration. One expects such designs to have evolved naturally in the biological world. For example, on the scale of insects, where capillary effects are critical [13], both designs could be useful: tubes with appropriate splays can either facilitate fluid uptake (*e.g.* in drinking through a proboscis), or prevent drop penetration into other body parts and so promote water-repellency. Nature raises related problems of spontaneous capillary-driven fluid motion in other geometries. For example, nectar is drawn mouthward along the tongues of hummingbirds through the action of surface tension [14]. Moreover, capillary feeding in shorebirds, though physically distinct in that it relies critically on contact angle hysteresis and boundary motion [7], may also benefit from beak flexure and beak splay [15] for reasons that have yet to be made clear.

Appendix

We here consider the general case of tubes with inner radius $a(z) = \delta + \alpha z + \beta z^2$. The force $F(z)$ acting on the drop can again be calculated and compared to the drop weight, from which we can deduce a phase diagram analogous to fig. 5. We show in fig. 7 the (δ, β)-plane of such a diagram, for $\alpha = 1.5°$ and $\Omega = 3\,\mathrm{mm}^3$. The three zones are similar to those in fig. 5. In zones I and III, a drop is unstable: it either slides downwards (in zone I) or climbs upwards (in zone III). Equilibrium is only possible in zone II. The principal difference with fig. 5 is the marked diminution of the stable zone II: at small β (left of point A), one now passes directly from zone III to zone I by increasing δ: there is no intervening stable equilibrium. This emphasizes the destabilizing effect of the
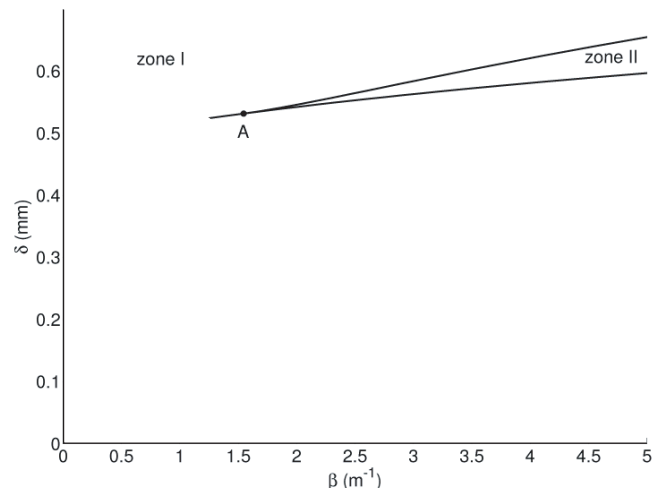

Fig. 7: Calculated stability diagram of wetting drops of volume $\Omega = 3\,\mathrm{mm}^3$ in a trumpet-shaped tube of inner radius $a(z) = \delta + \alpha z + \beta z^2$, with $\alpha = 1.5°$, and inclined at $30°$ relative to the horizontal. In zone III, the drop climbs. In zone I, it slides downwards. A stable-equilibrium position only arises in zone II. Note that the zone of stability is diminished relative to that evident in fig. 5 (obtained for $\alpha = 0$): to the left of point A, no stable-equilibrium height exists.

opening angle α. The coordinates of point A may be found by solving the system of equations $2\pi\kappa^{-2}\alpha\delta^2 + 2\kappa^{-2}\beta\Omega - \pi\sin\varphi\delta^4 = 0$ and $-\pi\delta^3\beta + \pi\alpha^2\delta^2 + \beta\Omega\alpha = 0$. We note that increasing α shifts the point A to the right, and so further diminishes the zone of stability.

REFERENCES

[1] Hauksbee F., *Philos. Trans.*, **27** (1712) 395.
[2] Bouasse H., *Capillarité et Phénomènes Superficiels* (Librairie Delagrave, Paris) 1924.
[3] Lorenceau É. and Quéré D., *J. Fluid Mech.*, **510** (2004) 29.
[4] Weaire D. and Drenckhan W., *Adv. Colloid Interface Sci.*, **137** (2008) 20.
[5] Rubega M. A. and Obst B. S., *Auk*, **110** (1993) 169.
[6] Estrella S. M., Masero J. A. and Perez-Hurtado A., *Auk*, **124** (2007) 1244.
[7] Prakash M., Quéré D. and Bush J. W. M., *Science*, **320** (2008) 931.
[8] Kusakov M. M. and Nekrasov D. N., *Dokl. Akad. Nauk URSS*, **119** (1958) 107.
[9] Reyssat M., Courbin L., Reyssat E. and Stone H. A., *J. Fluid Mech.*, **615** (2008) 335.
[10] Tsori Y., *Langmuir*, **22** (2006) 8860.
[11] Tsori Y., *Langmuir*, **23** (2007) 8028.
[12] Bico J. and Quéré D., *J. Fluid Mech.*, **467** (2002) 101.
[13] Bush J. W. M., Hu D. and Prakash M., *Adv. Insect Physiol.*, **34** (2008) 117.
[14] Kingsolver J. G. and Daniel T. L., *Oecologia*, **60** (1983) 214.
[15] Estrella S. M. and Masero J. A., *J. Exp. Biol.*, **210** (2007) 3757.